

BOOSTING UNKNOWN-NUMBER SPEAKER SEPARATION WITH TRANSFORMER DECODER-BASED ATTRACTOR

Younglo Lee¹, Shukjae Choi¹, Byeong-Yeol Kim¹, Zhong-Qiu Wang², Shinji Watanabe²

¹42dot Inc., Seoul, Korea

²Language Technologies Institute, Carnegie Mellon University, Pittsburgh, USA

younglo.lee@42dot.ai

ABSTRACT

We propose a novel speech separation model designed to separate mixtures with an unknown number of speakers. The proposed model stacks 1) a dual-path processing block that can model spectro-temporal patterns, 2) a transformer decoder-based attractor (TDA) calculation module that can deal with an unknown number of speakers, and 3) triple-path processing blocks that can model inter-speaker relations. Given a fixed, small set of learned speaker queries and the mixture embedding produced by the dual-path blocks, TDA infers the relations of these queries and generates an attractor vector for each speaker. The estimated attractors are then combined with the mixture embedding by feature-wise linear modulation conditioning, creating a speaker dimension. The mixture embedding, conditioned with speaker information produced by TDA, is fed to the final triple-path blocks, which augment the dual-path blocks with an additional pathway dedicated to inter-speaker processing. The proposed approach outperforms the previous best reported in the literature, achieving 24.0 and 23.7 dB Δ SI-SDR on WSJ0-2 and 3mix respectively, with a single model trained to separate 2- and 3-speaker mixtures. The proposed model also exhibits strong performance and generalizability at counting sources and separating mixtures with up to 5 speakers.

Index Terms— Speech separation, transformer, deep learning.

1. INTRODUCTION

Speech separation (SS) is the task of separating concurrent speech sources in a mixture signal recorded when multiple speakers talk simultaneously into individual speech signals. Although humans exhibit a remarkable capability of perceiving any target sound of interest from a mixture of multiple sound sources, researchers have found it challenging to enable machines to have the same hearing capability, especially in monaural conditions [1]. Thanks to the strong modeling capabilities of deep neural networks (DNN), significant advances have been made in SS. Since deep clustering [2–4], deep attractor network [5, 6], and permutation invariant training (PIT) [7, 8] successfully solved the label-permutation problem in talker-independent speaker separation, many subsequent studies [9–18] have developed more efficient DNN architectures to improve the separation performance. Through years of effort, the current state-of-the-art performance on the WSJ0-2mix dataset [2, 3], which is a popular benchmark designed for two-speaker separation, has reached an impressive scale-invariant signal-to-distortion ratio (SI-SDR) improvement of 23.5 dB over the mixture [16, 17].

In many early studies, it is commonly assumed that the number of speakers within each mixture is known and fixed, which drastically limits the application range of their developed systems. In order to overcome this limitation, [19–23] have proposed recursive

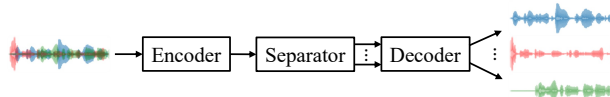


Fig. 1: High-level system illustration of SepTDA.

multi-pass source separation schemes. Meanwhile, [24–26] have proposed alternative approaches by training individual components for all conceivable numbers of speakers and at run time selecting one of the trained components, corresponding to the right number of speakers, to produce target estimates. However, their works require extra speaker identity information [20, 23], recursive separation steps [19, 21, 22], or multiple models [24–26]. Recently, encoder-decoder attractor (EDA) calculation-based methods have emerged, which are originally designed to handle an unknown number of speakers in speaker diarization [27], and demonstrated strong performance in SS [28–30].

Inspired by the above successful achievements, we propose SepTDA, a speech separation model that combines the strengths of the triple-path approach [28, 30] and an LSTM-augmented self-attention block (denoted as LSTM-attention), which can more efficiently capture local and global contextual information. In addition, a TDA calculation module is proposed with modifications to the original EDA [27] to effectively handle the undetermined count of speakers. We show that SepTDA outperforms the previous best reported in the literature by achieving state-of-the-art results on all the WSJ0-mix benchmark datasets [2, 3, 24], which consist of mixtures with two to five speakers. We share the separation samples¹.

2. PROPOSED METHOD

The proposed SepTDA, illustrated in Fig. 1, is based on a time-domain encoder-decoder separation framework [10]. Given a time-domain T -sample mixture $\mathbf{x} = \sum_{c=1}^C \mathbf{y}_c \in \mathbb{R}^T$ with C speakers, a separation model is trained to estimate each speaker source \mathbf{y}_c . SepTDA consists of an encoder, a separator, and a decoder. This section describes each of them.

2.1. Encoder

The encoder is a one-dimensional (1D) convolutional layer with a kernel size of L samples and a stride size of $L/2$ samples. It maps the mixture signal \mathbf{x} to a D_e -dimensional latent representation $\mathbf{E} \in \mathbb{R}^{T' \times D_e}$, where $T' = \lceil 2 \times T/L \rceil$ with proper zero-padding:

$$\mathbf{E} = \text{GELU}(\text{Conv1D}(\mathbf{x})), \quad (1)$$

where $\text{GELU}(\cdot)$ denotes the Gaussian error linear unit activation function [31].

¹<https://42speech.github.io/septda>

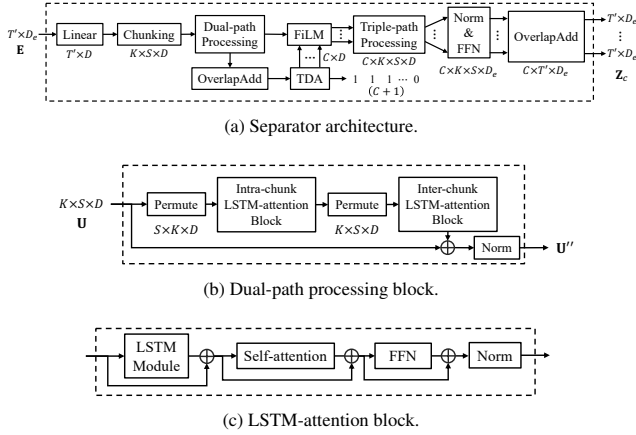


Fig. 2: Architectures of proposed (a) separator; (b) dual-path block; and (c) LSTM-attention block for intra- and inter-chunk processing

2.2. Separator

The separator takes the encoder output \mathbf{E} as input and produces C source representation $\mathbf{Z}_c \in \mathbb{R}^{T' \times D_e}$ where $c \in \{1, \dots, C\}$. The overall separator architecture is depicted in Fig. 2(a). \mathbf{E} is first fed into a linear layer with D output units, and then split into chunks of K frames with a hop size of $\lceil K/2 \rceil$, following [11]. This operation generates S equal-size chunks $\mathbf{U}^s \in \mathbb{R}^{K \times D}$ where $s \in \{1, \dots, S\}$. All chunks are stacked along a new chunk axis to obtain a three-dimensional tensor $\mathbf{U} \in \mathbb{R}^{K \times S \times D}$.

2.2.1. Dual-path processing

The segmented tensor \mathbf{U} is fed into a dual-path processing block depicted in Fig. 2(b):

$$\mathbf{U}' = [f_{\text{intra}}(\mathbf{U}[:, s, :]), \forall s] \in \mathbb{R}^{K \times S \times D}, \quad (2)$$

$$\mathbf{U}'' = \text{LN}([f_{\text{inter}}(\mathbf{U}'[k, :, :]), \forall k] + \mathbf{U}), \quad (3)$$

where $k \in \{1, \dots, K\}$ and $f_{\text{intra}}(\cdot)$, $f_{\text{inter}}(\cdot)$, and $\text{LN}(\cdot)$ are intra-, inter-chunk processing, and layer normalization, respectively. Instead of utilizing multiple blocks, a single block is employed for dual-path processing in our experiments. For f_{intra} and f_{inter} , we improve SepFormer [14] by incorporating an LSTM-augmented architecture, named LSTM-attention block, to better capture local and global contextual information with direct context-awareness [12]. The LSTM-attention block is illustrated in Fig. 2(c). The LSTM module consists of a layer normalization [32], followed by BLSTM [33] and a linear projection layer to transform back to the feature dimension D . Self-attention and feed-forward modules are the same as [14] except for the activation function (we replace the ReLU activation function with GELU). A residual connection is added after each module, followed by a layer normalization. Furthermore, in the self-attention module, we incorporate explicit positional information by employing T5-style relative position embeddings with per-head bias [34]. Unlike SepFormer [14], the LSTM-attention block does not require several transformer layers in each intra- or inter-chunk block. We tried to modify the order of the LSTM, self-attention, and FFN modules but did not observe any improvement.

2.2.2. Transformer decoder-based attractor calculation module

In previous studies that applied traditional EDA to SS [28, 29], an additional layer is needed to reduce the sequence length due to the fact that the LSTM encoder is not well-suited for handling extremely

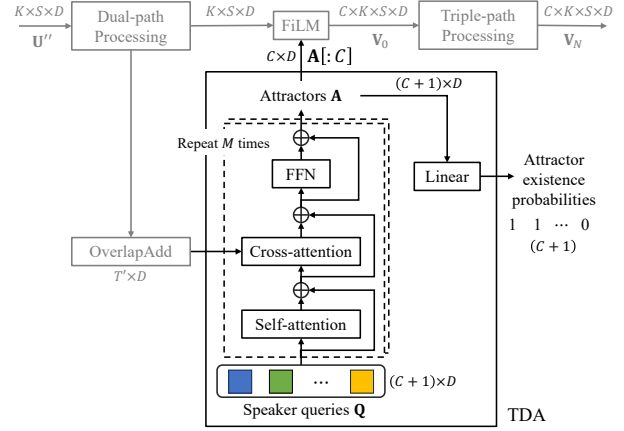


Fig. 3: Transformer decoder-based attractor calculation module.

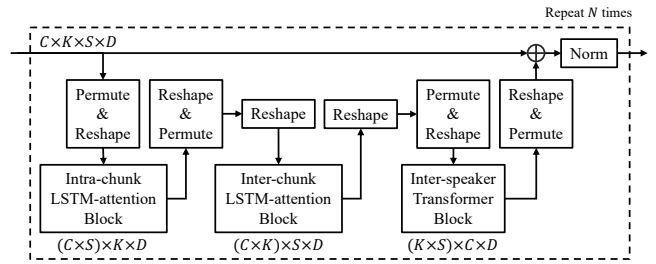


Fig. 4: Triple-path processing block.

long sequences. In addition, due to the nature of the LSTM encoder-decoder, EDA squashes all the information of input into a single fixed-length vector, which may yield a bottleneck in improving the performance [35]. In order to overcome these limitations, inspired by the idea of [27, 36], we propose a TDA calculation module by extending EDA to a transformer-based architecture.

The TDA calculation module, depicted in Fig. 3, consists of M transformer decoder layers. During training, the number of speakers C is assumed known, and $C + 1$ speaker query embeddings, $\mathbf{Q} \in \mathbb{R}^{(C+1) \times D}$, are randomly initialized and learned through the training process. TDA aims to estimate the attractors \mathbf{A} based on speaker queries \mathbf{Q} and mixture context as follows:

$$\mathbf{A} = \text{TDA}(\text{OverlapAdd}(\mathbf{U}''), \mathbf{Q}) \in \mathbb{R}^{(C+1) \times D}. \quad (4)$$

The context is obtained by employing the overlap-add operator to the dual-path processing output \mathbf{U}'' in Eq. (3) and is utilized as a context in cross-attention calculation, which enables to attend to the entire sequence with length T' , transforming each speaker query into a speaker-wise attractor. Note that the cross-attention operation has low complexity since C is much smaller than T' . We adopt masked self-attention in the TDA calculation module to prevent the c -th attractor prediction from attending to the next ($> c$) speaker queries. The first C attractors are responsible for speaker identification, while the last $(C + 1)$ -th attractor is utilized for estimating the speaker non-existence. The self-attention calculation in the first decoder layer is skipped as in [36]. After the TDA calculation, C speaker-wise attractors (denoted as $\mathbf{A}[:C]$) are combined with the dual-path processing output \mathbf{U}'' by feature-wise linear modulation (FiLM) conditioning [37], to generate 4-D tensor output \mathbf{V}_0 :

$$\mathbf{A}[:C] = [\mathbf{a}_1, \dots, \mathbf{a}_C] \in \mathbb{R}^{C \times D}, \quad (5)$$

$$\mathbf{V}_0 = \text{FiLM}(\mathbf{U}'', \mathbf{A}[:C]) \in \mathbb{R}^{C \times K \times S \times D}, \quad (6)$$

where $\text{FiLM}(\mathbf{F}, \mathbf{d}) = \text{Linear}(\mathbf{d}) \odot \mathbf{F} + \text{Linear}'(\mathbf{d})$ with two different linear projections of \mathbf{d} .

2.2.3. Triple-path processing

Following [28], \mathbf{V}_0 is refined by N triple-path processing blocks which extend the dual-path block with an additional inter-speaker transformer module. See Fig. 4 for an illustration. As in the previous dual-path processing, we use LSTM-attention blocks in the intra- and inter-chunk processing, while for the inter-speaker processing, a simple transformer layer is used since the order of speakers is not irrelevant due to the use of the PIT loss [8]. Residual connections are added after each processing block, followed by a layer normalization layer. The triple-path processing block is denoted as follows:

$$\mathbf{V}'_{n-1} = [f_{n,\text{intra}}(\mathbf{V}_{n-1}[c, :, s, :]), \forall c, s], \quad (7)$$

$$\mathbf{V}''_{n-1} = [f_{n,\text{inter}}(\mathbf{V}'_{n-1}[c, k, :, :]) \forall c, k], \quad (8)$$

$$\mathbf{V}_n = \text{LN}([f_{n,\text{speaker}}(\mathbf{V}''_{n-1}[c, :, :, :]), \forall c] + \mathbf{V}_{n-1}), \quad (9)$$

where $c \in \{1, \dots, C\}$ and $f_{n,\text{intra}}(\cdot)$, $f_{n,\text{inter}}(\cdot)$, and $f_{n,\text{speaker}}(\cdot)$ are respectively intra-chunk, inter-chunk, and inter-speaker processing in block $n \in \{1, \dots, N\}$.

After the final triple-path processed output \mathbf{V}_N is obtained, the overlap-add operation is employed on the S chunks, forming an output of size $\mathbb{R}^{C \times T' \times D}$, which has the same sequence length as the encoder output, \mathbf{E} . Then, layer normalization followed by a feed-forward layer with D_e output units is applied, producing $\mathbf{Z}_{N,c} \in \mathbb{R}^{T' \times D_e}$.

2.3. Decoder

The decoder reconstructs each source waveform $\hat{\mathbf{y}}_c$ from $\mathbf{Z}_{N,c}$ using the transposed convolution version of the encoder (i.e., with a kernel size of L samples and a stride size of $L/2$ samples) as follows:

$$\hat{\mathbf{y}}_{N,c} = \text{TransposedConv1D}(\mathbf{Z}_{N,c}). \quad (10)$$

2.4. Loss Functions

Inspired by [13, 24], a multi-scale loss technique is applied to our training objective. The reconstruction loss is computed from each output of triple-path processing block \mathbf{V}_n in Eq. (9). Then, the average over all the triple-path blocks is used as the loss. The reconstruction loss is defined by SI-SDR [9, 38] as follows:

$$\mathcal{L}_{\text{recon}} = -\frac{1}{N} \sum_{n=1}^N \max_{\pi \in \Pi_C} \frac{1}{C} \sum_{c=1}^C \text{SI-SDR}(\mathbf{y}_c, \hat{\mathbf{y}}_{n,\pi(c)}), \quad (11)$$

where N denotes the number triple-path blocks, Π_C is the set of all the permutations over C speakers and utterance-level PIT [8] is used to address the label-permutation problem, and $\hat{\mathbf{y}}_{n,c}$ is the estimated c -th source obtained from the n -th triple-path processing block output. Note that only the final output $\hat{\mathbf{y}}_{N,c}$ is used at inference time.

The training objective of the attractor existence probabilities is based on binary cross-entropy:

$$\mathcal{L}_{\text{attractor}} = \text{BCE}(\mathbf{a}, \sigma(\text{Linear}(\mathbf{A}))), \quad (12)$$

where \mathbf{A} is a set of attractor vectors in Eq. (4), $\mathbf{a} = [1, \dots, 1, 0]^T \in \mathbb{R}^{C+1}$, and $\sigma(\cdot)$ is the sigmoid activation function. $\text{BCE}(\cdot)$ denotes the binary cross entropy loss between target and input logits. Our final loss is $\mathcal{L}_{\text{total}} = \mathcal{L}_{\text{recon}} + \mathcal{L}_{\text{attractor}}$.

3. EXPERIMENTAL SETTINGS

3.1. Datasets

We evaluate SepTDA on popular SS benchmark datasets, WSJ0-{2,3,4,5}mix [2, 3, 24]. WSJ0-{2,3}mix [2, 3] are the most widely

used benchmark datasets in monaural speaker-independent SS tasks, which respectively consist of 2- and 3-speaker mixtures simulated based on clean speech signals in the WSJ0 corpus. Later, WSJ0-{4,5}mix with mixtures of 4 and 5 utterances are released by [24]. Unlike WSJ0-{2,3}mix, WSJ0-{4,5}mix have some mixtures with utterances from the same speaker. In these datasets, the relative level of a speech signal is randomly chosen from the range [0, 5] dB. Each dataset has 20000, 5000, and 3000 mixtures for training, validation, and testing, respectively, and the training and test sets do not share any speakers. The sampling rate is 8 kHz.

3.2. Experiment configurations

The encoder/decoder kernel size L in Section 2.1 and 2.3 is set to 16 with a stride size of 8 samples. The feature dimensions D_e and D in Section 2.3 are set to 256 and 128, respectively. For dual-path chunking, our model processes chunks of length $K = 96$ in Section 2.2 with 50% overlap. The number of TDA decoder layers M in Section 2.2.2 and triple-path blocks N in Section 2.2.3 is set to 2 and 8 respectively, and the number of hidden units in BLSTM is set to be 256 in each direction. We use 4 attention heads and an expansion factor of 4 for the feed-forward module.

Following [28], SepTDA is trained with three different dataset combinations: 1) WSJ0-2mix only, 2) WSJ0-{2,3}mix combined, and 3) WSJ0-{2,3,4,5}mix combined. We denote the three models as SepTDA₂, SepTDA_{2/3}, and SepTDA_[2-5], respectively. In contrast to [28], all the models are trained from scratch without using any data augmentation.

The AdamW optimizer [39] is used with an initial learning rate of 4×10^{-4} . The learning rate is halved when a validation loss has stopped improving for 5 successive epochs. We clip the L_2 norm of the gradients to 5. The batch size is set to 2 and the length of each training example is set to 4 seconds during training.

3.3. Evaluation metrics

SI-SDR improvement (Δ SI-SDR) [38] and SDR improvement (Δ SDR) [40] are used as the evaluation metrics. Following [28], we also consider two scenarios when evaluating SepTDA_{2/3} and SepTDA_[2-5], depending on whether the number of speakers is known or not. When it is unknown, the estimated number of speakers, \hat{C} , may not necessarily match the ground truth C . When there is an overestimation of the number of speakers (i.e., $\hat{C} > C$), we select the estimated sources corresponding to the initial C speaker queries. In cases of an underestimation in the number of speakers (i.e., $\hat{C} < C$), a silence signal (i.e., an all-zeros signal) is used as the estimate for the speakers that were not estimated as in [28]. Since the SI-SDR and SDR metrics are undefined if the reference signal is all-zero (i.e., $\log(0)$ is undefined), an epsilon value of 10^{-8} is used for the final log calculation, resulting in an SI-SDR value of -80 dB. The average mixture SI-SDR scores of 2 to 5mix are respectively 0, -3.2 , -5.0 , and -6.3 dB.

4. EVALUATION RESULTS

We analyze SepTDA by training it on different combinations of datasets and comparing its performance with previous studies. Then, we discuss the advantages of SepTDA through ablation studies.

Table 1: Comparison with previous models on WSJ0-2mix. TF and Q-Dual denote time-frequency and quasi-dual-path, respectively. '**' denotes the utilization of data augmentation (e.g., dynamic mixing or speed perturbation).

Models	Domain	Path	#params (M)	Δ SI-SDR (dB)	Δ SDR (dB)
DPRNN [11]	Time	Dual	2.6	18.8	19.0
Gated DPRNN [24]	Time	Dual	7.5	20.1	20.4
DPTNet [12]	Time	Dual	2.7	20.2	20.6
SepFormer [14]	Time	Dual	26.0	20.4	20.5
Wavesplit [13]	Time	Single	29.0	21.0	21.2
QDPN [15]	Time	Q-Dual	200.0	22.1	-
SepEDA ₂ * [28]	Time	Triple	12.5	21.2	21.4
MossFormer(L)* [18]	Time	Single	42.1	22.8	-
TF-GridNet [17]	TF	Dual	14.5	23.5	23.6
SepTDA ₂ with $L = 12$	Time	Triple	21.2	23.7	23.5
	Time	Triple	21.2	24.0	23.9

4.1. Results on WSJ0-2mix

Table 1 compares the separation performance of our models on WSJ0-2mix with previous systems in terms of Δ SI-SDR and Δ SDR. The SepTDA₂ model outperforms the current best reported in the TF-GridNet paper [17] by achieving a Δ SI-SDR of 23.7 dB. The performance is further improved to 24.0 dB by reducing the kernel size L introduced in Section 2.1 and 2.3 from 16 to 12 samples, at the cost of a marginal increase in the amount of computation (see the last row in Table 3).

4.2. Results on WSJ0-Cmix

Table 2 compares the results of SepTDA with previous systems which can separate mixtures with up to 3 or 5 speakers. Models marked as flexible C (by using \checkmark) are those that can specify the number of speakers to be separated, while the others can only separate a mixture into a fixed number of sources that they were trained with and require multiple models. For the models where the number of speakers is unknown, marked with '**', the speaker counting accuracy results are also reported. When the estimated attractor existence probability exceeds 0.5, we count it as an indication of the presence of a speaker, which is similar to Algorithm 1 of [28].

For the cases of 2 and 3 speakers, we observe that SepTDA outperforms the previous best systems by a large margin. Although the performance with an unknown number of speakers is slightly worse than that with a known number of speakers, it is better than the previous studies trained on the same dataset. SepTDA also performs the best when compared to studies that can separate up to 5 speaker sources. In particular, when the number of speakers is known, the performance degradation as the number of speakers increases is minimal compared to previous studies, and even for the 5mix dataset, Δ SI-SDR is not significantly different from the 2mix results of the previous studies. For an unknown number of speakers, although the speaker counting accuracy is lower than the previous SepEDA, we achieve much higher Δ SI-SDR. We could potentially improve speaker counting accuracy by stacking more layers instead of a single linear projection layer in Eq. (12), or by employing fine-tuning. However, we will leave these possibilities for future work.

4.3. Ablation results on LSTM-attention block

To study the effects of each module in SepTDA, we conduct an ablation study with a comparison with various baseline models. The results are reported in Table 3. DPRNN [11], Gated DPRNN [24], and SepFormer [14] are chosen as the baseline models because their architecture highly relies on BLSTM or Transformer layers. In addition, TF-GridNet [17], the current best model, is included and the computation cost is reported in terms of GMAC/s as in [17].

Table 2: Δ SI-SDR (dB) comparison on WSJ0-{2,3,4,5}mix. '**' denotes situations with an unknown number of speakers. Numbers in parentheses represent speaker counting accuracy in percentage.

Models	Flexible C	2	3	4	5
SepFormer [14]	\times	20.4	17.6	-	-
Wavesplit [13]	\times	21.0	17.3	-	-
MossFormer(L) [18]	\times	22.8	21.2	-	-
SepEDA _{2/3} [28]	\checkmark	21.5	19.9	-	-
SepTDA _{2/3}	\checkmark	24.0	23.7	-	-
SepTDA _{2/3} *	\checkmark	24.0 _(99.97)	22.8 _(97.93)	-	-
Recursive SS [21]	\checkmark	14.8	12.6	10.2	-
Gated DPRNN [24]	\times	20.1	16.9	12.9	10.6
Gated DPRNN* [24]	\times	18.6	14.6	11.5	10.4
SepEDA _[2-5] [28]	\checkmark	21.1	18.6	14.7	12.1
SepEDA _[2-5] * [28]	\checkmark	21.1 _(99.80)	18.4 _(97.00)	14.4 _(90.17)	11.6 _(96.87)
SepTDA _[2-5]	\checkmark	23.6	23.5	22.0	21.0
SepTDA _[2-5] *	\checkmark	23.6 _(99.90)	22.1 _(95.93)	19.5 _(90.10)	16.9 _(83.23)

Table 3: Ablation results on LSTM-attention block based on WSJ0-2mix.

# Models	Masking/Mapping	#params (M)	Δ SI-SDR (dB)	GMAC/s
1 DPRNN [11]	Masking	2.6	18.8	42.2
2 Gated DPRNN [24]	Mapping	7.5	20.1	31.5
3 SepFormer [14]	Masking	26.0	20.4	59.5
4 TF-GridNet [17]	Mapping	14.5	23.5	231.1
5 LSTM-attention	Masking	17.0	21.4	36.2
6 LSTM-attention	Mapping	17.0	22.0	36.2
7 w/o self-attention	Mapping	16.0	20.9	34.1
8 w/o LSTM	Mapping	13.0	20.0	31.1
9 SepTDA ₂	Mapping	21.2	23.7	81.0
10 with $L = 12$	Mapping	21.2	24.0	107.7

For a fair comparison with the baseline models, the proposed models are trained using WSJ0-2mix. For LSTM-attention (from row 5 to 8), the TDA module and triple-path processing are excluded for a fair comparison, and 8 dual-path processing blocks are stacked as in other dual-path approaches [11, 14, 24]. For row 5, masking is performed in the encoded embedding space and ReLU is used for encoder activation and mask estimation as in [14].

From the results in row 5 and 6, direct mapping shows better results than the masking method. This aligns with the findings in TF-GridNet [16, 17]. The model in row 6 yields the most favorable separation performance while achieving a harmonious balance of model size between Gated DPRNN and SepFormer. Row 7 and 8 also show the advantages of using the self-attention module and the LSTM module, respectively. Note that, in the model of row 8, the embedding dimension D introduced in Section 2.2 is increased to 256 in order to maintain the total number of parameters as similar as possible, and the resulting model can be seen as a lightweight version of SepFormer.

5. CONCLUSIONS

We have proposed SepTDA, a monaural speech separation model that can handle mixtures with an unknown number of speakers. We have proposed an improved LSTM-attention block to the previous dual- and triple-path processing blocks. In addition, the proposed TDA module infers the relations of a set of learned speaker queries and the mixture context and directly generates individual attractors for each speaker. By combining these strengths together, SepTDA achieves state-of-the-art results on all the datasets examined in this paper. Even when the number of speakers is unknown, SepTDA shows strong performance and generalizability at separating mixtures with up to 5 speakers.

6. REFERENCES

- [1] Y.-m. Qian, C. Weng, X.-k. Chang, S. Wang *et al.*, “Past review, current progress, and challenges ahead on the cocktail party problem,” *Frontiers of Information Technology & Electronic Engineering*, vol. 19, no. 1, pp. 40–63, 2018.
- [2] J. R. Hershey, Z. Chen, J. Le Roux, and S. Watanabe, “Deep Clustering: Discriminative embeddings for segmentation and separation,” in *Proc. ICASSP*, 2016, pp. 31–35.
- [3] Y. Isik, J. Le Roux, Z. Chen, S. Watanabe *et al.*, “Single-channel multi-speaker separation using deep clustering,” in *Proc. Interspeech*, 2016, pp. 545–549.
- [4] Z.-Q. Wang, J. Le Roux, and J. R. Hershey, “Alternative objective functions for deep clustering,” in *Proc. ICASSP*, 2018, pp. 686–690.
- [5] Z. Chen, Y. Luo, and N. Mesgarani, “Deep attractor network for single-microphone speaker separation,” in *Proc. ICASSP*, 2017, pp. 246–250.
- [6] Y. Luo, Z. Chen, and N. Mesgarani, “Speaker-independent speech separation with deep attractor network,” *IEEE/ACM Trans. Audio, Speech, Lang. Process.*, vol. 26, no. 4, pp. 787–796, 2018.
- [7] D. Yu, M. Kolbæk, Z.-H. Tan, and J. Jensen, “Permutation invariant training of deep models for speaker-independent multi-talker speech separation,” in *Proc. ICASSP*, 2017, pp. 241–245.
- [8] M. Kolbæk, D. Yu, Z.-H. Tan, and J. Jensen, “Multi-talker speech separation with utterance-level permutation invariant training of deep recurrent neural networks,” *IEEE/ACM Trans. Audio, Speech, Lang. Process.*, vol. 25, no. 10, pp. 1901–1913, 2017.
- [9] Y. Luo and N. Mesgarani, “TasNet: Time-domain audio separation network for real-time, single-channel speech separation,” in *Proc. ICASSP*, 2018, pp. 697–700.
- [10] —, “Conv-TasNet: Surpassing ideal time-frequency magnitude masking for speech separation,” *IEEE/ACM Trans. Audio, Speech, Lang. Process.*, vol. 27, no. 8, pp. 1256–1266, 2019.
- [11] Y. Luo, Z. Chen, and T. Yoshioka, “Dual-Path RNN: Efficient long sequence modeling for time-domain single-channel speech separation,” in *Proc. ICASSP*, 2020, pp. 46–50.
- [12] J. Chen, Q. Mao, and D. Liu, “Dual-path transformer network: Direct context-aware modeling for end-to-end monaural speech separation,” in *Proc. Interspeech*, 2020, pp. 2642–2646.
- [13] N. Zeghidour and D. Grangier, “Wavesplit: End-to-end speech separation by speaker clustering,” *IEEE/ACM Trans. Audio, Speech, Lang. Process.*, vol. 29, pp. 2840–2849, 2021.
- [14] C. Subakan, M. Ravanelli, S. Cornell, M. Bronzi *et al.*, “Attention is all you need in speech separation,” in *Proc. ICASSP*, 2021, pp. 21–25.
- [15] J. Rixen and M. Renz, “QDPN - Quasi-dual-path network for single-channel speech separation,” in *Proc. Interspeech*, 2022, pp. 5353–5357.
- [16] Z.-Q. Wang, S. Cornell, S. Choi, Y. Lee *et al.*, “TF-GridNet: Making time-frequency domain models great again for monaural speaker separation,” in *Proc. ICASSP*, 2023, pp. 1–5.
- [17] —, “TF-GridNet: Integrating full- and sub-band modeling for speech separation,” *IEEE/ACM Trans. Audio, Speech, Lang. Process.*, vol. 31, pp. 3221–3236, 2023.
- [18] S. Zhao and B. Ma, “MossFormer: Pushing the performance limit of monaural speech separation using gated single-head transformer with convolution-augmented joint self-attentions,” in *Proc. ICASSP*, 2023, pp. 1–5.
- [19] K. Kinoshita, L. Drude, M. Delcroix, and T. Nakatani, “Listening to each speaker one by one with recurrent selective hearing networks,” in *Proc. ICASSP*, 2018, pp. 5064–5068.
- [20] J. Shi, J. Xu, G. Liu, and B. Xu, “Listen, think and listen again: Capturing top-down auditory attention for speaker-independent speech separation,” in *Proc. IJCAI*, 2018, pp. 4353–4360.
- [21] N. G. Naoya Takahashi, Sudarsanam Parthasarathy and Y. Mitsufuji, “Recursive speech separation for unknown number of speakers,” in *Proc. Interspeech*, 2019, pp. 1348–1352.
- [22] J. Shi, X. Chang, P. Guo, S. Watanabe *et al.*, “Sequence to multi-sequence learning via conditional chain mapping for mixture signals,” in *Proc. NIPS*, vol. 33, 2020, pp. 3735–3747.
- [23] J. Shi, J. Xu, Y. Fujita, S. Watanabe *et al.*, “Speaker-conditional chain model for speech separation and extraction,” in *Proc. Interspeech*, 2020, pp. 2707–2711.
- [24] E. Nachmani, Y. Adi, and L. Wolf, “Voice separation with an unknown number of multiple speakers,” in *Proc. ICML*, 2020, pp. 7121–7132.
- [25] J. Zhu, R. A. Yeh, and M. Hasegawa-Johnson, “Multi-decoder DPRNN: Source separation for variable number of speakers,” in *Proc. ICASSP*, 2021, pp. 3420–3424.
- [26] S. E. Chazan, L. Wolf, E. Nachmani, and Y. Adi, “Single channel voice separation for unknown number of speakers under reverberant and noisy settings,” in *Proc. ICASSP*, 2021, pp. 3730–3734.
- [27] S. Horiguchi, Y. Fujita, S. Watanabe, Y. Xue *et al.*, “End-to-end speaker diarization for an unknown number of speakers with encoder-decoder based attractors,” in *Proc. Interspeech*, 2020, pp. 269–273.
- [28] S. R. Chetupalli and E. A. P. Habets, “Speech separation for an unknown number of speakers using transformers with encoder-decoder attractors,” in *Proc. Interspeech*, 2022, pp. 5393–5397.
- [29] S. Maiti, Y. Ueda, S. Watanabe, C. Zhang *et al.*, “EEND-SS: Joint end-to-end neural speaker diarization and speech separation for flexible number of speakers,” in *Proc. SLT*, 2023, pp. 480–487.
- [30] S. R. Chetupalli and E. A. P. Habets, “Speaker counting and separation from single-channel noisy mixtures,” *IEEE/ACM Trans. Audio, Speech, Lang. Process.*, vol. 31, pp. 1681–1692, 2023.
- [31] D. Hendrycks and K. Gimpel, “Gaussian error linear units (GELUs),” *arXiv preprint arXiv:1606.08415*, 2016.
- [32] J. Ba, J. R. Kiros, and G. E. Hinton, “Layer normalization,” *arXiv preprint arXiv:1607.06450*, 2016.
- [33] S. Hochreiter and J. Schmidhuber, “Long short-term memory,” *Neural computation*, vol. 9, no. 8, pp. 1735–1780, 1997.
- [34] C. Raffel, N. Shazeer, A. Roberts, K. Lee *et al.*, “Exploring the limits of transfer learning with a unified text-to-text transformer,” *J. Mach. Learn. Res.*, vol. 21, no. 1, 2020.
- [35] D. Bahdanau, K. Cho, and Y. Bengio, “Neural machine translation by jointly learning to align and translate,” in *Proc. ICLR*, 2015.
- [36] N. Carion, F. Massa, G. Synnaeve, N. Usunier *et al.*, “End-to-end object detection with transformers,” in *Proc. ECCV*, 2020, pp. 213–229.
- [37] E. Perez, F. Strub, H. de Vries, V. Dumoulin *et al.*, “FiLM: Visual reasoning with a general conditioning layer,” in *Proc. AAAI*, 2018.
- [38] J. Le Roux, S. Wisdom, H. Erdogan, and J. R. Hershey, “SDR – half-baked or well done?” in *Proc. ICASSP*, 2019, pp. 626–630.
- [39] I. Loshchilov and F. Hutter, “Decoupled weight decay regularization,” in *Proc. ICLR*, 2018.
- [40] E. Vincent, R. Gribonval, and C. Févotte, “Performance measurement in blind audio source separation,” vol. 14, no. 4, pp. 1462–1469, 2006.